JOURNAL OF MATERIALS SCIENCE 27 (1992) 1672–1682

Dielectric properties of humid mica surfaces

N. BANO*, A.K. JONSCHER
Physics Department, Royal Holloway and Bedford College, Egham Hill, Egham, Surrey, TW20 0EX, UK

The dynamic behaviour of conduction and polarization processes on humid surfaces of mica has been studied in the frequency and time domains as function of the relative humidity, sample geometry, steady bias and electrode material. Detailed analysis of complex impedance and admittance plots has led to improved understanding of the role of the electrodes. The general conclusion which confirms and augments earlier studies is that humid mica surfaces may be represented by a parallel combination of an essentially extraneous "electrode capacitance" which does not depend on humidity and bias, and the surface processes which ultimately become dominated by low-frequency dispersion. It is concluded that the behaviour does not depend in a major way on the nature of the electrode material, which implies that the dispersive processes observed are intrinsic to the humid surface, and are not dominated by contact effects between the metal contacts and the humid surface.

1. Introduction

The phenomena of surface conduction on humid hydrophyllic surfaces have been extensively studied in terms of so-called "direct current" or steady state processes [1], but they have received relatively little attention from the standpoint of their dynamic behaviour as manifesting itself in the frequency or time dependence of the surface currents. As early as 1914, Curtis reported measurements of the a.c. response of humid glass and observed that the conductance increased exponentially with the relative humidity (RH), especially above 50%. Lachish and Steinberger [2] found an exponential dependence of surface resistance on the radial spacing of concentric electrodes. Yager and Morgan [3] made measurements on borosilicate glass in the frequency range 1–100 kHz and found a similar rise with RH as did Curtis. In the different but related context of open-circuit voltages found in metal–insulator sandwiches, Ieda *et al.* [4] explained these in terms of electrochemical processes.

The study of the time-domain (TD) response of humid surfaces by Jonscher and Ramdeen [5] was crucial to the advancement of our understanding of the mechanisms involved, by establishing the fact that the discharge currents were independent of the amplitude, V_a, of the applied bias, while the charging currents were increasing linearly with V_a.

A more recent study was made by Owede and Jonscher [6] of humid mica, glass and silicon nitride surfaces, who used a modern frequency response analyser in the frequency range 10^{-3}–10^{4}Hz and the corresponding time-domain (TD) instrument to look at the charging and discharging currents. They gave detailed results for a range of RH and for a wide range of electrode geometries in terms of their aspect ratio, s/l, as explained in Fig. 1. Their results confirmed the earlier observations of exponential dependence of surface conductance on RH while the availability of much lower frequencies revealed a strong low-frequency dispersion (LDF) dominating the low-frequency end of their spectral range. The strongly non-linear dependence of surface conductance on the aspect ratio of the electrodes s/l suggested clearly the non-uniformity of current distribution on the surface.

The present study was undertaken to extend the earlier work [6] with the added element of higher sensitivity of the current–time measuring system, with more emphasis on the role of electrode material and with the introduction of impedance/admittance analysis to elucidate more clearly the nature of the surface transport process. This appeared to us to be important because the phenomenon of low-frequency dispersion, so widely observed in transport on humid insulating surfaces, remains poorly understood and more information is required to enable one to form a clear picture. Among the main points requiring elucidation are the nature of the electrochemical interactions and the possible relation between LFD and non-uniform distribution of current on the surface-filamentation.

2. Low-frequency dispersion

Low-frequency dispersion (LFD) was established relatively recently by Jonscher as a specific limiting form of the "universal" dielectric response [7–9]. In LFD the real and imaginary components of the complex dielectric susceptibility, $\tilde{\chi}(\omega) = \tilde{\varepsilon}(\omega) - \varepsilon_\infty = \chi'(\omega) - i\chi''(\omega)$, follow a fractional power law of the form

$$\chi''(\omega) \propto \cot(n\pi/2)\chi'(\omega) \propto \omega^{n-1} \quad (1)$$

* Permanent address: Physics Department, University of Karachi, Karachi 75270, Pakistan.

0022–2461

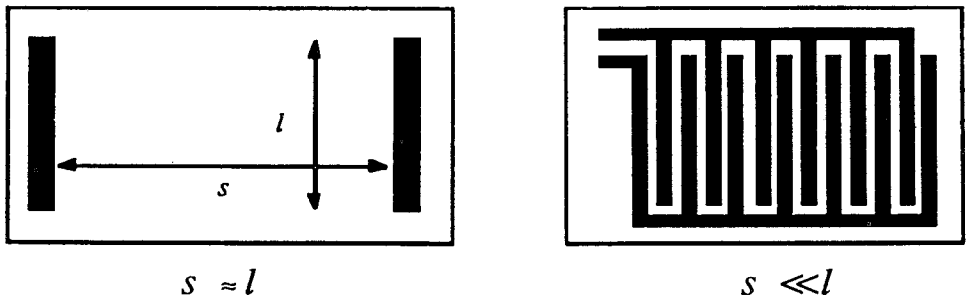

Figure 1 The arrangement of surface electrodes defining their separation s and length l, for two different geometries.

where the exponent n is small compared with unity, typically 0.1–0.3. Here $\tilde{\varepsilon}(\omega)$ is the complex permittivity and ε_∞ is a suitable " high-frequency limit" where the processes in question do not cause any more losses. Similar relations obtain for the complex capacitance $\tilde{C}(\omega)$ and the susceptibility equivalent $\tilde{X}(\omega) = \tilde{C}(\omega) - C_\infty$ which are more convenient when one is not certain if the processes involved relate to volume or to interfaces.

The power-law Relation 1 implies a rapid rise of both components of $\tilde{\chi}(\omega)$ and $\tilde{C}(\omega)$ towards low frequencies, their ratio remaining constant with $\chi'(\omega) \ll \chi''(\omega)$, corresponding to a very lossy system. This is shown schematically in Fig. 2a where LFD region with a small exponent $n = n_2$ is followed at higher frequencies by a less lossy power-law response with $n = n_1$ closer to unity.

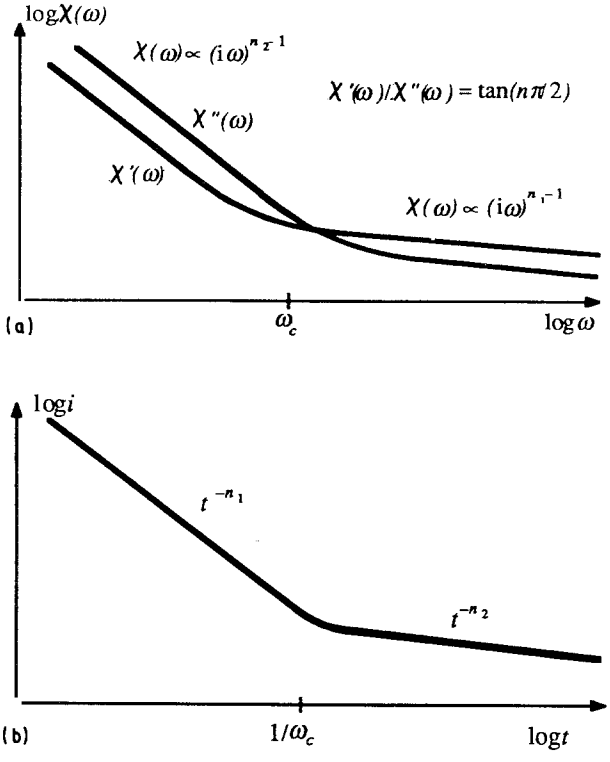

Figure 2 (a) A schematic presentation of the frequency-domain behaviour of a system showing LFD behaviour with the characteristic parallelism in the logarithmic plots of the real and imaginary components of the complex susceptance, $X'(\omega)$ and $X''(\omega)$, respectively. The high-frequency region corresponds to the normal low-loss behaviour of dielectrics, the low-frequency dispersive region is the LFD phenomenon. (b) The corresponding time-domain behaviour, with the long-time almost constant current corresponding to the low-frequency dispersive part of (a).

A complementary aspect of the LFD process is the time dependence of the charging and discharging currents under step-function potential excitation which are the Fourier transforms of the power-law Relation 1 and which are themselves fractional power laws

$$i(t) \propto t^{-n} \tag{2}$$

which in the present case of small values of n_2 corresponds to very slowly decreasing current with time, as shown in Fig. 2b.

The alternating current conductance of a system is defined as

$$G(\omega) = \omega X''(\omega) \propto \omega^n \tag{3}$$

which in the case of LFD rises very slowly with frequency and may therefore be easily mistaken for direct current (d.c.) conductance. The crucial test here is the behaviour of $C'(\omega)$ which should be constant for d.c. flow and varies rapidly for LFD.

3. Method of presentation of results

Our experimental results are presented in three modes:

(a) as logarithmic plots of $C'(\omega)$ and $C''(\omega)$ which give a very clear aspect of the low-frequency behaviour, although they cease to be informative once the pure LFD behaviour is complicated by other phenomena as will be seen later;

(b) as complex admittance plots $\tilde{Y} = i\omega\tilde{C}$ which are useful in sorting out parallel elements in the response;

(c) as logarithmic time-domain plots of charging currents $i_c(t)$ and discharging currents $i_d(t)$.

We have also used complex impedance plots $\tilde{Z} = \tilde{Y}^{-1}$ which emphasize the series elements in the response, but we have found these to be less informative and not corresponding to the physical situation.

Because of their linear representation, the $\tilde{Y}$ plots have to be suitably magnified in the low-frequency region if we are to obtain a proper assessment of the LFD behaviour. This is where the frequency plots (a) are very valuable.

4. Experimental procedure

Sheets of Muscovite and Ruby mica were cleaved to a thickness of approximately 0.1 mm with a view to minimizing bulk conduction processes. Our experience shows that there were no significant differences between different types of mica and this is consistent with earlier observations by Owede and Jonscher [6]

who found that the response of humid surfaces was very similar in all hydrophyllic materials such as mica and glass. The samples were cleaned with 4-methyl pentone-2-one, rinsed with distilled water and dried. This method was adopted to clean samples which had been cleaved earlier, but experiments carried out on untreated freshly cleaved surfaces have given essentially similar results. Electrodes were applied by evaporation or painting from suspensions of metallic particles in organic solvents, their geometry being as shown in Fig. 1 which defines the electrode spacing s and their length l. The aspect ratio s/l was varied between 0.008 and 2.

Small painted silver dots were placed on some samples along the inter-electrode space to enable potential measurements to be made during the charging process. These measurements showed conclusively that the potential is dropped fairly uniformly along the sample length and is not dropped predominantly at the electrodes, as would be the case if the entire behaviour was dominated by the contacts. This point was already treated in detail previously [6] and we do not give any data for it.

Frequency domain measurements were taken on a Solartron frequency response analyser (FRA) with a Chelsea dielectric interface to adapt the instrument to high impedances. Time-domain measurements were made on a Chelsea time-domain instrument with logarithmic current amplifier covering a current range 10^{-12}–10^{-3}A and a logarithmic time range 10^{-4} –10^{3} s.

Samples were placed in a desiccator under controlled relative humidity (RH) [10] and were kept for 36 h before commencement of measurements, which was found to be sufficient to reach steady state conditions under given humidity. In general, measurements were commenced with 97% RH and subsequent runs were made at 33%, 66%, 75% and again at 97% RH and it was found that, for the most part, the final results were close to the initial ones, although the lower-frequency data were generally slightly higher. Subsequent cycling between low and high RH produced only very slight upward drift of capacitance and the same was observed when the sample was simply kept at a constant RH for extended periods of time, typically days on end. No ultimate saturation of response could be observed even after 30 days. Likewise, prolonged exposure to laboratory air would cause a gradual upward drift $\tilde{C}(\omega)$ data, say by a factor of 2 at low frequencies. The amount of drift was larger for short, wide samples, i.e. small s/l ratios. No recovery of the initial response could be achieved by baking at 100°C under vacuum for 1 h.

This ageing process is doubtless caused by slow irreversible chemical interaction between the mica surface and water but attempts to make this visible on scanning electron micrographs were unsuccessful. This ageing process is most likely accelerating with RH. As a consequence of this lack of stability it was difficult to obtain fully consistent results for consecutive runs on the same sample with, say, variable RH or bias voltage. Likewise, measurements on different samples with variable s/l ratios were fraught with some random errors which made exact comparisons difficult.

The opposite trend to ageing was observed following prolonged (1 week) exposure to steady bias which caused $\tilde{C}(\omega)$ data measured subsequently without bias to fall initially by a factor of between 5 and 10, but a waiting period of 1 week, or so, would restore the original response, subject to the ageing process mentioned above.

5. Results and discussion

5.1. The shape of capacitance –frequency plots

The logarithmic plots of $\tilde{C}(\omega)$ show the characteristic strong dispersion towards low frequencies which was reported previously [6] but the parallelism of $C'(\omega)$ and $C''(\omega)$ expected for ideal LFD is not always observed, as was already noted but not explored further there. This is so because of the complicating features of competing parallel processes, as will be seen in the admittance diagrams. Fig. 3 gives three typical sets of data, two of these corresponding to

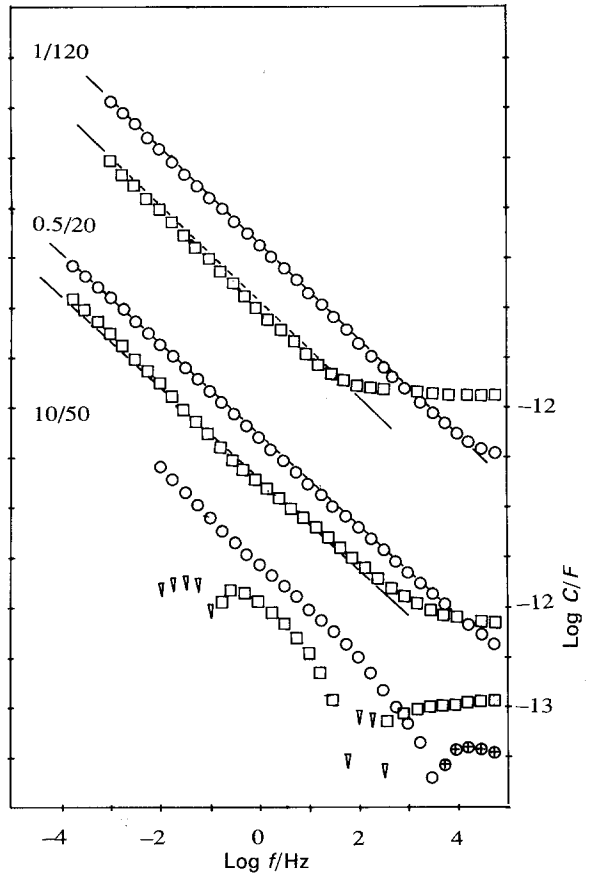

Figure 3 Three typical examples of the dependence of $C'(\omega)$ for (□) positive and (▽) negative values, and (○) $C''(\omega)$ for different geometries and biases, plotted on a common basis of log ω and displaced vertically for clarity. The amplitude of the a.c. signal is 1 V, all three samples are at 97% RH. The upper plot corresponds to the shortest sample, $s = 1$, $l = 120$ mm and to 1V steady bias, the middle one to $s = 0.5$, $l = 20$ and zero bias, and the lowest one to a long sample $s = 10$, $l = 50$ and zero bias. The upper two plots correspond to a nearly perfect LFD behaviour over five to six decades of frequency with Karmers–Kronig compatible lines drawn for comparison, the lowest one is severely distorted.

nearly ideal LFD, although there are visible deviations from the perfect parallelism of the real and imaginary components, the third one giving a strongly distorted picture due to the effect of parallel elements.

5.2. Impedance –admittance plots

The $C(\omega)$ plots are particularly useful for bringing out the LFD properties, but their interpretation becomes progressively more difficult as other processes become important, so that we propose to concentrate on admittance plots instead. In the analysis of our data in terms of admittance and impedance it became obvious that the former showed clear evidence of a stray capacitance dominating the high-frequency behaviour. This capacitance which will be referred to as C_1, is easily identifiable with the electrode capacitance which has to be regarded on physical grounds as being in parallel with the remaining processes. This consideration rules out the impedance representation as the correct interpretation of our data.

5.3. The general appearance of admittance plots

Typical surface admittance plots for humid mica, glass and other hydrophyllic insulators look as shown schematically in Fig. 4a with a steep straight line spur, Y_1, at high frequencies, followed at lower frequencies by a more or less distorted circular arc, Y_2, and finishing at the lowest frequencies by a nearly horizontal branch which may have one of two shapes shown in the enlarged inset (b).

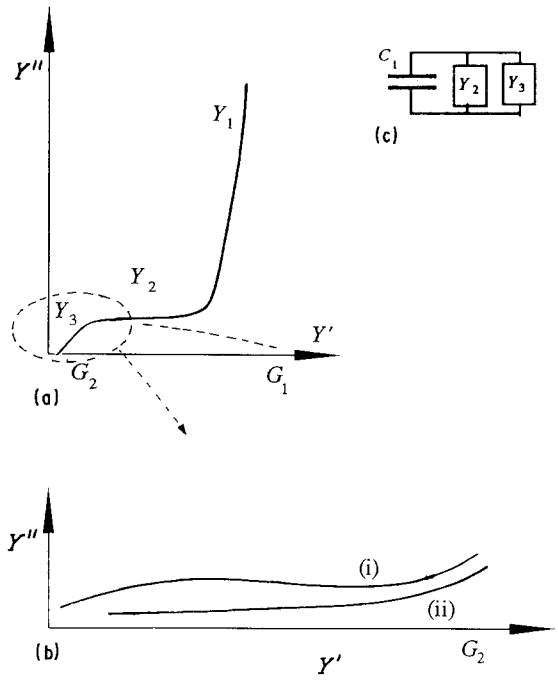

Figure 4 (a) The appearance of a typical surface admittance plot showing three principal regions: the high- frequency nearly vertical straight line Y_1, the intermediate arc Y_2 and the low-frequency component Y_3 which is not always sufficiently resolved, and the shape of which in considerable enlargement appears as in (b) where two alternative shapes (i) and (ii) are shown. The significance of the dotted contour in (a) is explained in the text. (c) The corresponding equivalent circuit.

The steeply rising branch, Y_1, corresponds to an almost pure capacitance and it is possible to conclude that it represents a "stray" capacitance C_1 of the electrode system plus any other strays. This is naturally a pure loss-free capacitor and the inclination arises from an interaction between this admittance and that of the high-frequency end of Y_2.

We note the following points about the capacitance C_1:

(a) its value is around 0.1 – 1 pF which is reasonable under the circumstances;

(b) it is independent of the bias, humidity and electrode material;

(c) its value is proportional to l/s for large values of this ratio, short, wide samples, and is almost independent of l/s for smaller values.

All these points confirm the attribution of C_1 to stray electrode capacitance.

The frequency dependence of Y_1 follows fairly faithfully the frequency dependence of a pure capacitor but its finite inclination arises from an interaction with the residual high-frequency components of Y_2 and this may be checked by carrying out a subtraction. There remains some uncertainty as to the exact shape of the residual admittance Y_2 because there is no unique way of resolving this subtraction, but on the whole a fairly good approximation may be obtained by taking the best fit to the frequency dependence of the high-frequency branch which usually shows whether or not the residual values fall on the real axis. As a general point it should be noted that a purely real value could only be independent of frequency and, therefore, in the frequency range in question the Y_1 plot ought to be vertical, which it normally is not up to the highest measured frequencies.

The low-frequency part of Y_2 is difficult to resolve on the scale used in Fig. 4a and is shown in considerable enlargement in Fig. 4b. The prevailing trend, insofar as it is actually accessible in the available frequency range, is clearly of the type of low-frequency dispersion (LFD) and it may show one of two general shapes denoted by (i) and (ii). The former is a distinctive shallow arc and it must correspond to a series combination of a resistance and an LFD element, the latter is a more or less straight line heading for the origin and it must correspond to a pure LFD element without any series resistance.

Denoting by G_1 the intercept on the Y' axis defined by the high-frequency end of Y_1, this also defines the high-frequency end of Y_2. Fig. 5 gives the collected data for G_1 and C_1 against the aspect ratio s/l for all samples measured by us. Allowing for the scatter of data resulting from the non-reproducibility discussed above, we note that C_1 falls with s/l for smaller values of this ratio and tends to saturate for larger values. This may be understood on the basis of the fact that the geometrical capacitance of the contacts ought to be proportional to l/s but at the lower end the influence of extraneous strays becomes dominant.

We also note that $G_1 \propto l/s$ to a rather better approximation than C_1, thereby confirming that this part may be attributed to the same inter-electrode

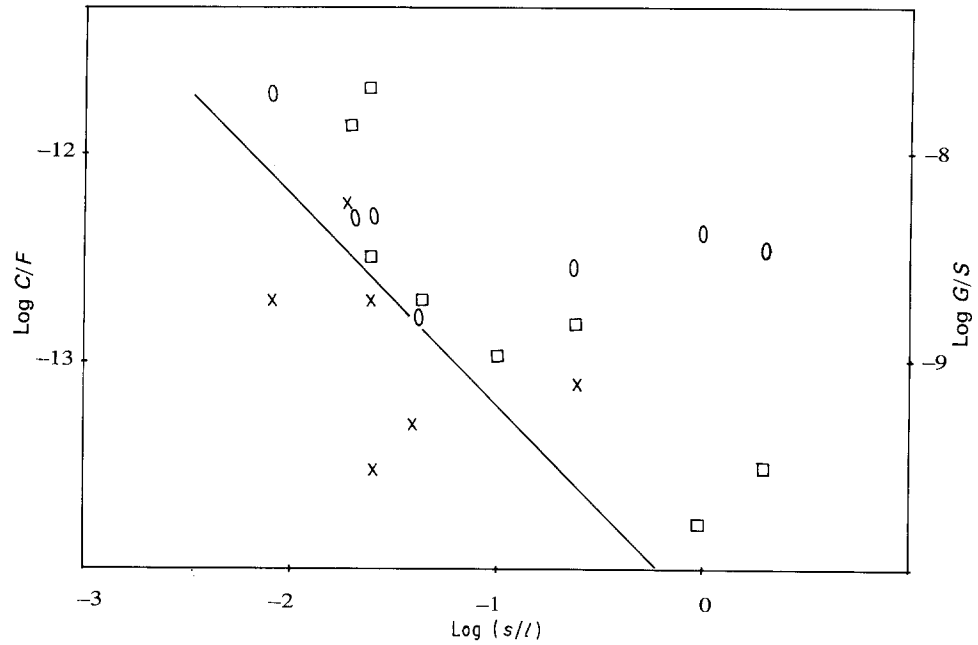

Figure 5 The dependence of (0) the capacitance C_1 and of the conductances (□) G_1 and (×) G_2 on the aspect ratio s/l for all samples investigated. The values of G_2 are fraught with some uncertainty because of the difficulty of defining precisely where the boundary lies between the higher-frequency arc and the onset of the LFD. The line l/s is drawn for reference.

space, with the simplifying feature that there is no "stray" element as in C_1.

The undoubted presence of the LFD element at the low-frequency end of the spectrum is well confirmed by the strong dispersion visible on the plots of $C'(\omega)$ and $C''(\omega)$, typically in Figs. 3 and 11. It may also be seen clearly in the inversion into the complex impedance plane which emphasizes this part of the plot, but we do not give any examples of this in the interest of brevity.

Denoting by G_2 the intercept on the Y' axis at the low-frequency end of Y_2 before the onset of LFD we note that $G_2 \propto l/s$, albeit with some considerable scatter which may be attributed to the fact that this end of the spectrum is often not well resolved and that the precise position of the intercept is sometimes not easily determined. These are also shown in Fig. 5.

The shape of the complex plot of Y_2 is shown schematically in Fig. 6 and we note two possible alternatives, of which one gives a definite limit of the admittance at G_1 and the other where no such limit is in evidence. The circular arc at the lowest frequencies corresponds in the admittance plane to a nearly pure capacitance in series with some other element but our ability to discern more detail about this is limited. It would be plausible to regard the series capacitor as representing some "contact" property of the inter-electrode space.

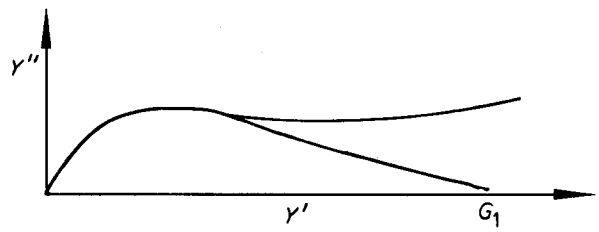

Figure 6 The shape of the complex plane plot of Y_2 after the subtraction of the capacitance C_1 and of the LFD component Y_3. There are two possible shapes, one in which the plot goes to the real axis at G_1 and the other where there is a continuing rise.

To illustrate these points and, in particular, to show how an even small deviation from parallelism in the $C'(\omega)$ and $C''(\omega)$ plots is reflected in the complex $\tilde{Y}$ plots, we show in Figs 7 and 8 the admittance data for the same samples as are shown in the upper two sets in Fig. 3. Fig. 7 shows an evident irregularity in the transition from the LFD region to the higher-frequency region, which we are unable to explain. However, there is no doubt about the presence of the LFD and the line drawn through the points goes through the origin, suggesting that no d.c. conduction can be resolved in this instance. In Fig. 8, on the other hand, the transition from the low- to the high-frequency region is more gradual and there is some fine structure in the lowest frequency region which might indicate the presence of a series resistance in the system. It should be stressed, however, that despite the fact that the data go down nearly to 10^{-4}Hz it is not possible to resolve the LFD behaviour in sufficient detail.

It is desirable to remove the dominant influence in the $\tilde{Y}$ plots arising from the essentially extraneous capacitance C_1 by subtracting $i\omega C_1$ from the overall admittance in an attempt to reveal the true shape of the surface admittance $\tilde{Y}_2$, as indicated schematically in Fig.6. Here an uncertainty arises because it is not possible to know the exact value of C_1 to be used – too small an estimate will result in a rising branch of $\tilde{Y}_2$, too large will lead to negative values of Y''_2. It would appear that a choice in which the $\tilde{Y}_2$ has remained nearly horizontal over the high-frequency region is close to the true situation, as shown in Fig. 9 for two samples. Whatever the detailed shape of $\tilde{Y}_2$, however, it is evidently relatively "flat" at high frequencies and approximates to a strongly inclined arc at low frequencies before going over into LFD. It is not possible

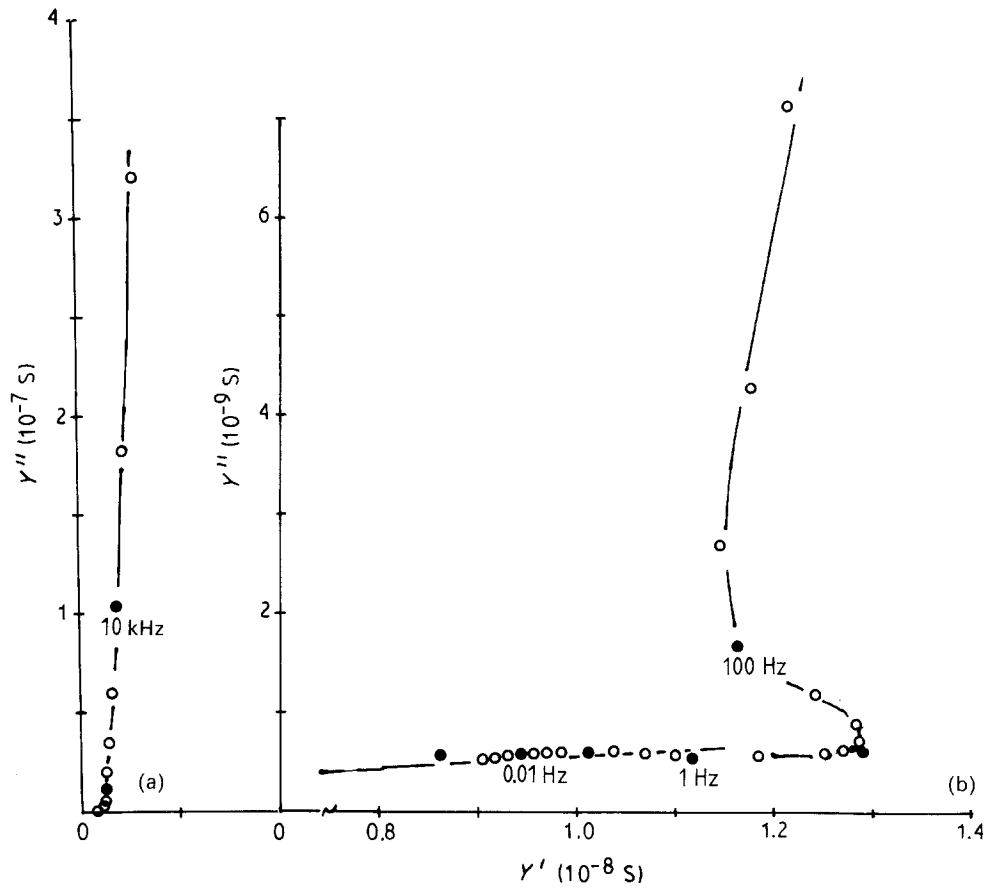

Figure 7 The admittance of the short sample with $s/l = 1/120$, RH = 97%, the same as the one shown in Fig. 3, (a) giving the complete data; (b) the enlarged part at low frequencies, to show the complications resulting in the deviations from ideal LFD behaviour in Fig. 3. Note the false zero on the Y' axis which may produce a misleading impression. The sloping line in the lower part of (b) goes through the true zero, indicating pure LFD.

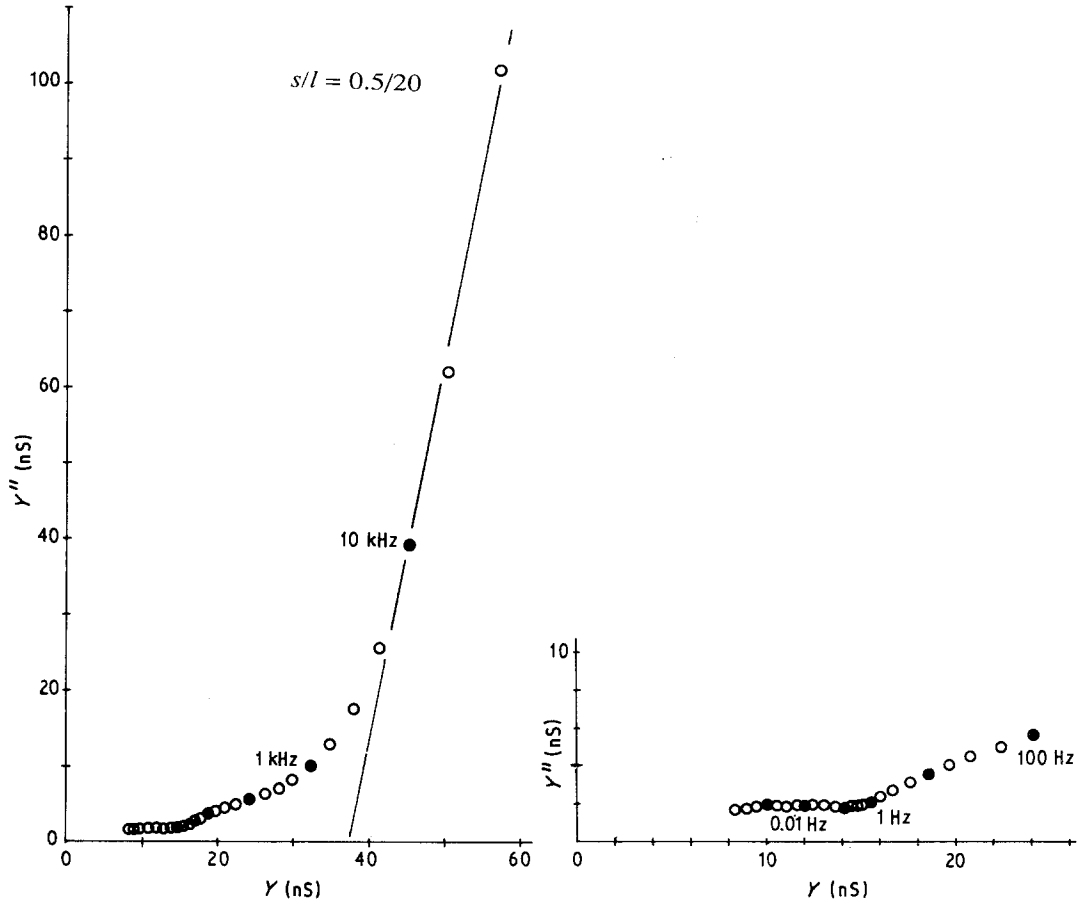

Figure 8 The admittance of the second sample shown in Fig. 3 with $s/l = 0.5/20$. The main plot gives the complete data, the inset shows the enlarged part at low frequencies indicating the absence of a clear-cut LFD behaviour but leaving no doubt about the strong dispersion. Some fine structure is evident at the lowest frequencies.

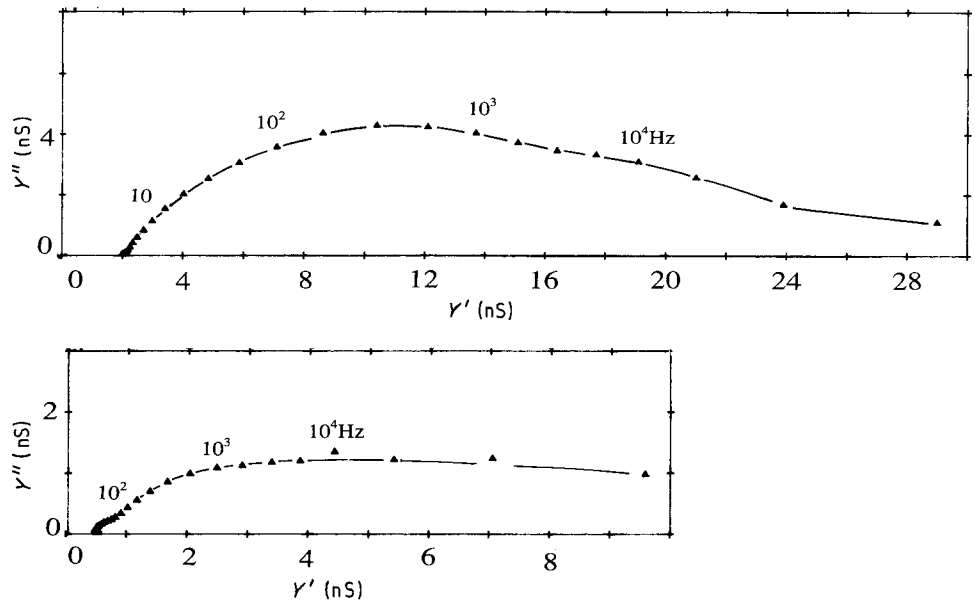

Figure 9 Two examples of subtraction of the high-frequency component, $i\omega C_1$, from the admittance plot to reveal the surface admittance, $\tilde{Y}_2$. The choice of C_1 was made so as to avoid either crossing over to negative values of Y''_2 or a rising branch, because this is believed to lead to the most likely shape of $\tilde{Y}_2$. The strongly elongated shape of the plot should be noted.

to speculate now on the full significance of this result other than pointing out that it does not follow any simple "equivalent circuit".

5.4. Series or parallel LFD ?

The question may be asked whether the LFD in the low-frequency limit is a parallel or a series process, because it appears as a clear feature both in $\tilde{Z}$ and $\tilde{Y}$ plots. The physical significance of the difference is that in the series model the LFD property belongs to some contact which dominates over the response of the inter-electrode space, while in the parallel model the LFD behaviour emerges as a long-time transport-dominated process which coexists with the high-frequency processes in the inter-electrode space [6, 11]. The problem is resolved by noting that a series LFD is unlikely to dominate the dielectric behaviour of the inter-electrode space which is not, by its nature, highly conducting in its own right. Thus, in our opinion, the parallel model is much more plausible.

5.5. Humidity dependence

The relative humidity (RH) of the ambient air has a very strong effect on surface admittance, changing the loss component by orders of magnitude compared with the dry condition, although the capacitance, C_1, remains little affected. In common with other situations such as the bulk conductance in humid media [10], and also in surface conductance in humid sand [8] and in mica paper [12], the strong dependence of the LFD component on RH begins at some 60% –70% RH and it becomes approximately exponential as shown in Fig. 10.

The full frequency dependence of $C'(\omega)$ and $C''(\omega)$ for the same sample at different RH is shown in Fig. 11. We note that even at the lowest RH of 14 % there is a measurable dispersion below 10 Hz, presumably due to chemisorbed water which cannot be driven out without baking the system. Strong dispersion sets in at 66% and becomes fully developed at 97%. The high-frequency value $C'(\omega)$ remains unaffected, as stated above.

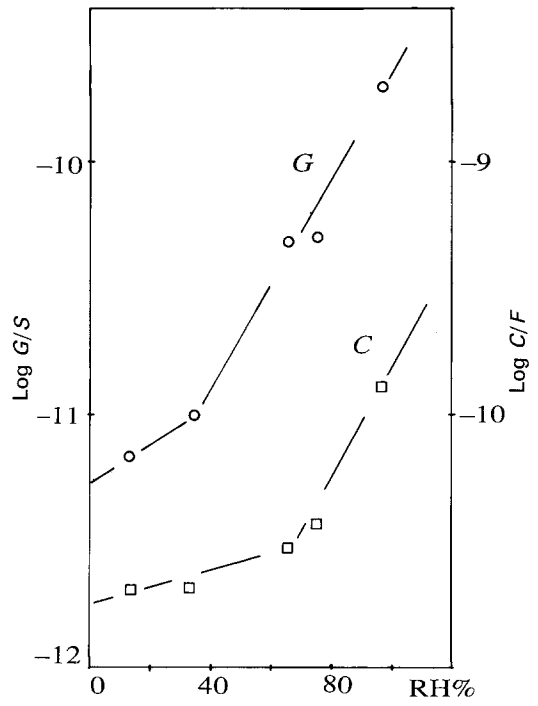

Figure 10 The dependence of the conductance (○) $G = \omega C''(\omega)$ and (□) $C'(\omega)$ on RH, showing the exponential tendency. The conductance values are almost independent of frequency in the LFD region and both C' and G were taken at 0.1 Hz.

Exposure of mica and glass to humidity always causes some irreversible changes so that it is not possible to return exactly to the pristine condition, even after baking and this must be attributed to some chemical changes taking place on the surface of a humid hydrophyllic material.

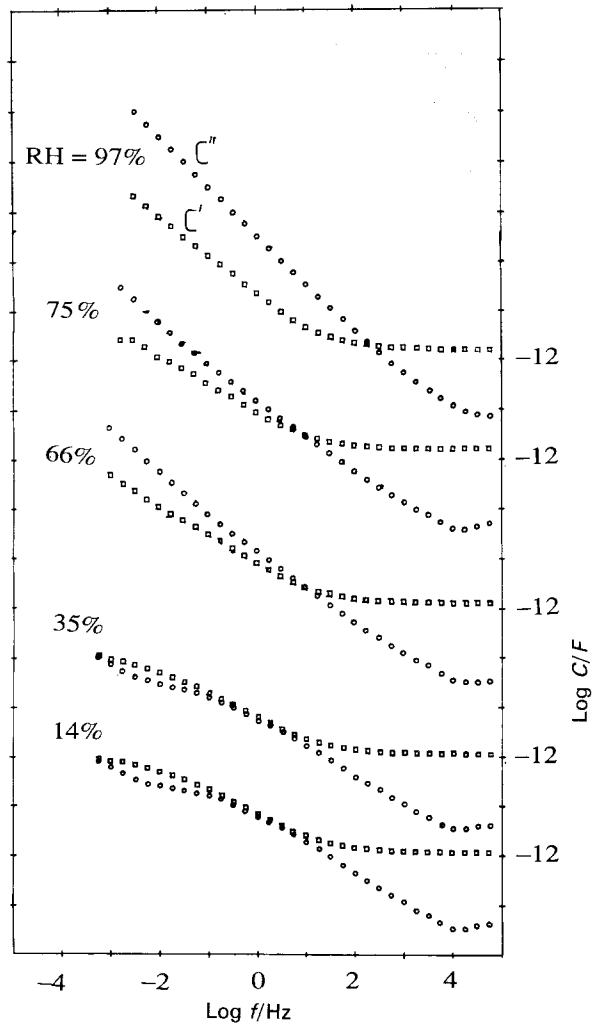

Figure 11 The evolution of the frequency dependence of the complex capacitance of a sample with $s/l = 1/120$ with rising RH. The consecutive sets corresponding to rising RH are displaced vertically by two decades for clarity. The two sets for 24 and 35% are virtually identical, the onset of strong dispersion becomes apparent above 60%. Note that the high-frequency response is unaffected.

5.6. The effect of electrode material

The material of the electrodes has some effect on the low-frequency branch of the $\tilde{Y}$ plots while leaving unchanged the high-frequency branch. We have tried several electrode materials, some painted from organic suspensions and some evaporated. The broad characteristics are shown in Table I and it should be stressed that these are based on a relatively narrow range of samples, so that they should not be taken as definitive properties.

TABLE I Influence of electrode material on the admittance of humid mica

Material	Comments
Au evaporated	Extensive LFD with evidence of series resistance and fine structure
Al evaporated	Strong LFD with some parallel conductance, rather irregular high-frequency behaviour
Ag evaporated	Similar to Au
Ag painted	Similar to evaporated Ag but anomalous LFD
Cu evaporated	Similar to Al with strong LFD but with regular high-frequency behaviour as in Ag and Au
Carbon painted	Simple behaviour, less evidence of LFD

The general impression from our results is, nevertheless, that the effect of different electrode materials on the admittance characteristics is not all that drastic, especially when comparing the presumably very inert carbon or gold with the relatively very reactive aluminium. This conclusion is important because it supports other evidence from the present studies that any interaction between the material of the electrode and the humid surface is of secondary significance compared with the "intrinsic" properties of such humid surfaces themselves.

5.7. Bias dependence

Bias has only a very slight effect on the higher-frequency part of $\tilde{Y}$ while there is some effect on the low-frequency part, but it is impossible to specify precisely what this effect is. One reason for this is the lack of reproducibility of results and the lasting "memory" of previous biasing which makes it difficult to be sure which changes are the effects of different biases and which are accidental effects.

Long-term application of bias for hours and days tends to lower the absolute values of $|\tilde{Y}_2|$ in the low-frequency part without significantly changing the shape of the plot, and the effect takes a long-time (several days) to recover, although it is not possible to return completely to the orginal characteristic.

5.8. Time-domain response

We have investigated in detail the time-domain behaviour of both the charging currents, $i_c(t)$ and of the discharging current $i_d(t)$ under step-function voltage excitation of amplitude V_a. Most of our measurements were taken in the relatively slow time range of 10–10^3 s, although a few results obtained with our TD spectrometer are also included.

Fig. 12 gives the $i_c(t)$ and $i_d(t)$ data for the longest and shortest samples for a range of step amplitudes. The following properties are apparent.

1. The charging currents $i_c(t)$ show relatively "flat" time dependence, especially for the longer samples, while the discharging currents follow fractional power laws, especially for the longer samples with large s/l ratios. A finite slope of the $\log i$–$\log t$ plot is to be expected from the Fourier transform (Equation 2) but in the case of $i_c(t)$ there may be a "true d.c. component" making the resulting current much flatter. If this were subtracted the remaining part should be closer to $i_d(t)$ in both magnitude and time dependence.

2. We note the general property that $i_c(t)$ is larger or even much larger than $i_d(t)$, because $i_c(t)$ depends on V_a while $i_d(t)$ either does not at all or much more slowly. This is shown in Fig. 13 where the strong asymmetry of behaviour is evident. These results are in broad agreement with earlier data from Jonscher and Ramdeen [5] and Owede and Jonscher [6] and they show that the conventional modelling in terms of passive circuit components cannot be applicable and an electrochemical model is essential.

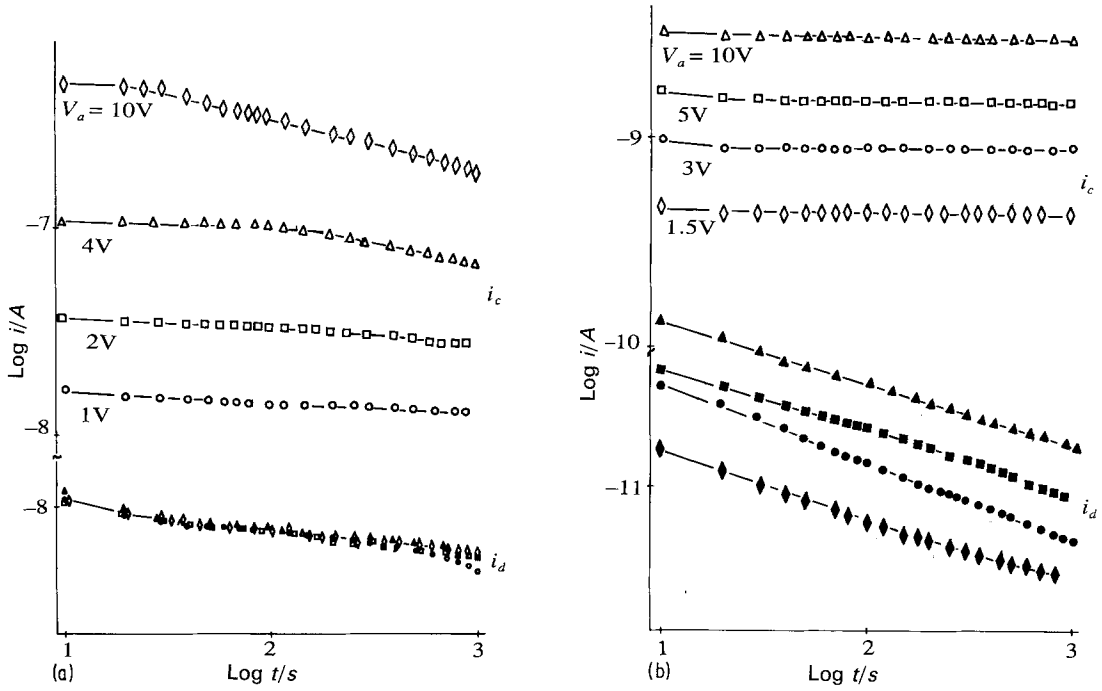

Figure 12 Examples of time dependence of $i_c(t)$ and $i_d(t)$ for the (a) shortest (1/120) and (b) longest (40/20) sample, RH = 97%. Both, but especially the latter, show varying degrees of weak time dependence.

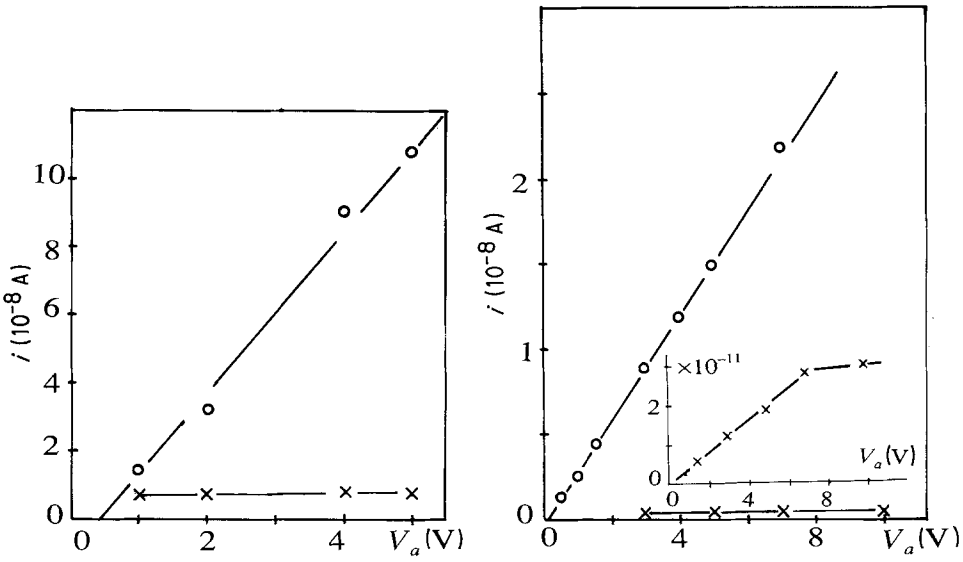

Figure 13 The dependence of the amplitude of (○)$i_c(t)$ and (X)$i_d(t)$ on V_a, showing a strongly asymmetric behaviour. The values of $i_c(t)$ and $i_d(t)$ were taken arbitrarily at 10 s but the precise choice of this time does not affect the broad trend of the results. The values of $i_d(t)$ for the longest sample 40/20 are two orders of magnitude smaller than $i_c(t)$ and are shown separately in the inset. The slow saturation with V_a should be noted. (a) R = 40 MΩ, s/l = 1/120, (b) R = 4 GΩ, s/l = 40/20. RH = 97%.

3. An interesting phenomenon is seen in the longest sample 40/20 at lower RH = 75% where the discharge current shows clear signs of "exhaustion" and the recovery takes progressively longer times with increasing charging voltage, V_a, Fig. 14. This phenomenon had been reported under similar conditions in humid zeolites by Jonscher and Haidar [13] and was attributed to a sweeping away of the active species which did not have time to be replenished from the atmosphere.

Fig. 15 shows an example of the more complete TD response of sample 1/50 for a range of charging voltages obtained with the automatic measuring system. The discharging currents show a clear slope instead of a purely constant current previously reported [5, 6] and a gradual saturation towards higher voltages.

6. Conclusions

The present study represents a significant step forward from the earlier work of Owede and Jonscher and it establishes certain principles governing the transport of ions on humid surfaces of hydrophyllic materials. In doing so, it clarifies a number of misconceptions and highlights the existence of some important unresolved questions.

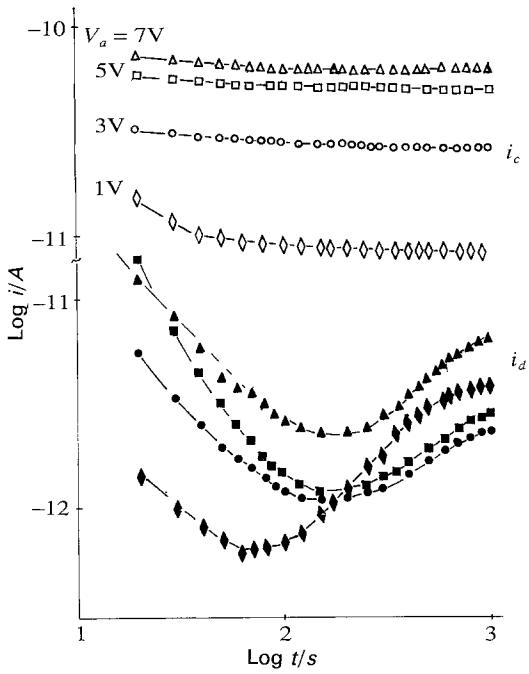

Figure 14 The behaviour of the long sample (40/20) under lower RH = 75%, showing clear signs of an "exhaustion" of the discharge process, taking an increasingly long time to recover and reach the higher equilibrium value as the step voltage is increased.

The most important results may be summarized as follows.

1. Surface transport shows a large degree of dependence on frequency and on time which distinguishes it from the conventional concept of d.c. conduction. The most important phenomenon is the low-frequency dispersion which dominates the behaviour at long times and low frequencies and which points clearly to the importance of electrochemical processes.

2. The electrical "contacts" to the humid surfaces made by metallic electrodes do not cause significant limitations to the transport, at least in the sense that they do not seem to cause any serious voltage drop.

3. The admittance of the humid surface proper, after subtracting the extraneous stray capacitance, presents a complicated picture which does not lend itself to simple interpretation in terms of classical capacitors and conductors and in which strongly dispersive processes seem to dominate even at relatively high frequencies. This represents one of the unresolved questions posed by the present study.

4. The detailed nature of the electrochemical interactions involved in surface transport is not very clear, but it is evident that they are not concentrated at the electrodes and must, therefore, be considered as being distributed along the surface.

5. We do not know enough about the detailed nature of the interactions between water and the surface of the hydrophyllic materials such as mica, but it is clear that there exist some irreversible and also some slowly reversible processes and these make it difficult to carry out fully reproducible measurements. However, the exponential dependence of the conductance on RH suggests clearly that we are dealing with some form of percolation process. In particular, we do not understand the reasons for the changes in surface impedance under the action of prolonged exposure to high humidity, nor to prolonged steady bias.

Although the present study was concerned entirely with humid surfaces of mica, we know that very similar results can be obtained with glass and also with silicon nitride. There are, therefore, good reasons for regarding the features of surface transport reported here as having more general validity than merely in the context of mica.

It may be said that there does not exist at present an agreed theoretical interpretation of the LFD behaviour in general and in a two-dimensional context, in particular. In view of the evident non-uniformity of

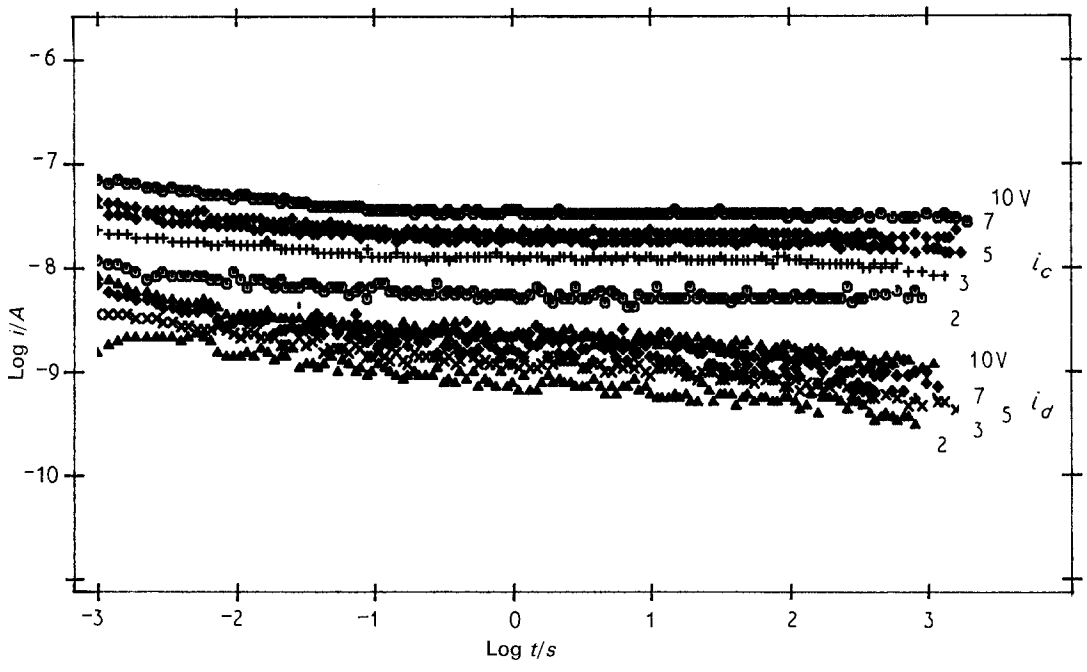

Figure 15 T-D response of sample 1/50 taken over six decades of time from 1 ms and for a range of charging voltages:1, 2, 3, 5, 7, 10 V. Note the slope of $\log i_d(t)$.

flow and its probable filamentary nature, it is tempting to consider the various fractal approaches – for an excellent discussion of the various possible models see Niklasson [14]. However, there is as yet insufficient experimental evidence for the detailed properties of our conducting surfaces to enable this analysis to be applied with conviction. The alternative approach based on the "energy criterion" argument proposed by Jonscher [9] has yet to be fully tested and generally accepted and likewise the concept of distributed electrochemical action has to be developed more clearly.

Acknowledgements

NB is indebted to the British Council for the award of a Scholarship and to the University of Karachi for study leave.

References

1. K. KAWASAKI, K. KANOU and Y. SEKITA, *J. Phys. Soc. Jpn* **13,** (1958) 222.
2. U. LACHISH and J. T. STEINBERGER, *J. Phys. D* **7**(1974) 58.
3. W. A. YAGER and S. O. MORGAN, *J. Phys. Chem.* **3** (1931) 2026.
4. M. IEDA, G. SAWA, S. NAKAMURA and Y. NISHIO, *J. Appl. Phys.* **46** (1976) 2796.
5. A. K. JONSCHER and T. RAMDEEN, *IEEE Trans.* **EI-22,** (1987) 35.
6. E. F. OWEDE and A. K. JONSCHER, *J. Electrochem. Soc.* **135,** (1988) 1757.
7. A. K. JONSCHER, *Phil. Mag.* **B38,** (1978) 587.
8. *Idem,*"Dielectric Relaxation in Solids" (Chelsea Dielectrics, London 1983).
9. *Idem, J. Mater. Sci.* **26** (1991) 1618.
10. A. R. HAIDAR and A. K. JONSCHER, *J. Chem. Soc. Faraday Trans.* 1 **82,** (1986) 3535.
11. M. A. CHAUDHRY and A. K. JONSCHER, *J. Mater. Sci.* **23** (1988) 208.
12. *Idem, ibid.* **20** (1985) 3581.
13. A. K. JONSCHER and A. R. HAIDAR, *J. Chem. Soc, Faraday Trans.* **1 82** (1986) 3553.
14. G. A. NIKLASSON, *J. Appl. Phys.* 62 (1987) R1.

Received 21 May
and accepted 28 May 1991